Communication

Size and Shape Control of Colloidally Synthesized IV#VI Nanoparticulate Tin(II) Sulfide

Stephen G. Hickey, Christian Waurisch, Bernd Rellinghaus, and Alexander Eychmu#ller

J. Am. Chem. Soc., **2008**, 130 (45), 14978-14980 • DOI: 10.1021/ja8048755 • Publication Date (Web): 16 October 2008

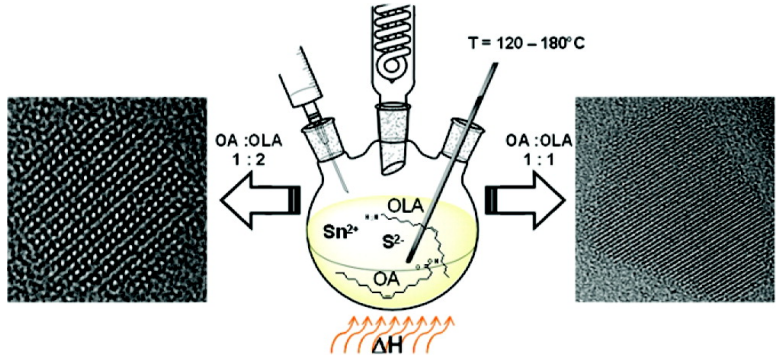

More About This Article

Additional resources and features associated with this article are available within the HTML version:

- Supporting Information
- Access to high resolution figures
- Links to articles and content related to this article
- Copyright permission to reproduce figures and/or text from this article

View the Full Text HTML

J|A|C|S
COMMUNICATIONS

Published on Web 10/16/2008

Size and Shape Control of Colloidally Synthesized IV−VI Nanoparticulate Tin(II) Sulfide

Stephen G. Hickey, Christian Waurisch, Bernd Rellinghaus, and Alexander Eychmüller*

Physical Chemistry/Electrochemistry, 01069 Dresden, IFW Dresden, P.O. Box 270116, D-01171, Dresden, Germany

Received July 29, 2008; E-mail: alexander.eychmueller@chemie.tu-dresden.de

At present the IV−VI series of semiconducting materials comprises a number of the most promising materials for IR applications.[1−4] The interest in these materials is primarily because they are narrow band gap materials and therefore have the potential to be employed in devices as optically active components in the near-infrared (NIR) and infrared (IR) spectral region and are hence beneficial to such applications as solar cells, detectors, telecommunications relays, etc. The interest in the IV−VI materials has also grown in recent years because of the observation that these materials can demonstrate efficient multiple exciton generation (MEG),[3,5−7] which is the ability to generate more than one electron−hole pair per high energy photon absorbed. This has implications for the efficiencies of solar cells and other applications based on these materials, especially as it provides a means by which the Shockley/Queisser efficiency limit may be overcome.

Tin sulfide is one of the four layered semiconductors (SnSe, GeS, and GeSe being the other members) which form an isomorphic subset of the IV−VI materials.[8] These materials possess an orthorhombic crystal structure (D_{2h}^{16}: *Pnma*) whose structure may be considered as a distorted NaCl structure. This type of structure is of particular interest owing to the arrangement of the cations and anions within the structural lattice. The layers of cations are separated only by van der Waals forces, which provide a chemically inert surface devoid of dangling bonds and surface density of states. Consequently, there is no Fermi level pinning at the semiconductor surface. This fact leads to a considerably high chemical and environmental stability.[9] These materials could therefore support the fabrication of highly mismatched solid-state junctions without interface states. Furthermore SnS has both an indirect and a direct bandgap (1.09 and 1.3 eV, respectively).[10] The direct bandgap, being very close to that of silicon, is located in the spectral region required of materials if they are to be efficient collectors of solar radiation and has a high optical absorption coefficient for photons with energies greater than 1.3 eV.[11] The absorption coefficient near the fundamental absorption edge is $\sim 10^4$ cm^{-1}, allowing light absorption at narrow thickness.[12] All these, in addition to the theoretical calculations by Prince[13] and Loferski[14] which indicate that SnS possesses all the qualities required for an efficient solar spectrum absorber, suggest that SnS is a suitable candidate for incorporation into clean energy conversion cells as well as a variety of other optoelectronic devices. It is also reported that, depending on the tin content, SnS may be *p*-type, *n*-type or change its conductivity upon heat treatment,[15] and studies have shown it has potential as a material in electrochemical capacitors in hybrid storage devices.[16] Other added benefits are that the component elements are abundant in nature and are low cost, as well as being chemically stable and nontoxic, placing it in an almost unique position as a semiconductor with the possible exception of FeS_2.

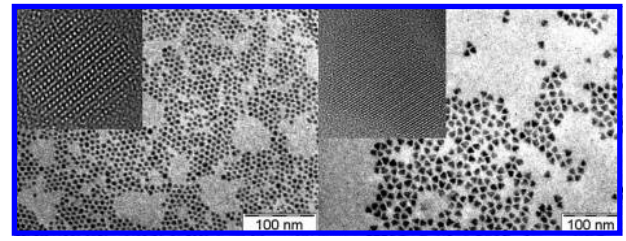

Figure 1. Overview and HRTEM images (insets) of spherical- and triangular-shaped SnS nanocrystals.

Initial attempts to use tin(II) acetate as a precursor and its subsequent conversion to tin(II) oleate resulted in large particulate material, which appears to possess a thin flake-like portion within which is located an elongated protrusion of approximately 200 nm along the longest axis (see Supporting Information: SI 1a). Shapes very similar to these have previously been reported[17] for a microwave-assisted growth procedure. However when Sn-[$N(SiMe_3)_2$]$_2$, (bis[bis(trimethylsilyl)amino]tin(II)) was employed as precursor for the tin oleate synthesis the reaction was observed to go to completion quickly, in agreement with other works.[18] The SnS synthesis is based on the reaction of thioacetamide with the tin(II) precursor in the presence of oleic acid. Thus, bis[bis(trimethylsilyl)amino]tin(II), trioctylphosphine (TOP), oleic acid (OA), and octadecene (ODE) were added to a 3-necked flask and heated to 170 °C under inert atmosphere. Into this mixture was then quickly injected a thioacetamide (1 mmol) solution in 10 mL (30.4 mmol) of oleylamine (OLA) and 3 mL (6.7 mmol) of TOP upon which the temperature was allowed to fall to 125 °C. The reaction temperature was maintained for between 3 and 5 min during which time the mixture was observed to change color from clear to dark red and then to brown, after which point it was cooled to room temperature. The resulting material was precipitated from solution using short-chained alcohols and was found to be redispersible in a number of organic solvents such as toluene and chloroform. To affect shape control the ratio of oleic acid to oleylamine in the reaction mixture was varied (see below).

The as-synthesized nanocrystals are monodisperse with a size distribution typically below 10% without the requirement of size-selective protocols. The crystalline structure of the SnS particles (see Supporting Information SI 2) can be indexed to that of the α-SnS, herzenbergite modification (JCPDS 39-354) which is orthorhombic (*Pbnm*, $a = 4.305$, $b = 11.262$, $c = 3.976$ Å).

The triangular particles also possess the herzenbergite structure as seen with the electron beam parallel to the [00-1] direction with the long *b*-axis being enlarged by some 7% with respect to a and c directions or vice versa). If one interprets the particle boundaries in the image as facets (which should be undertaken with caution) then the triangular particles are mainly terminated by {110} and {100} facets which are all facets containing both

10.1021/ja8048755 CCC: $40.75

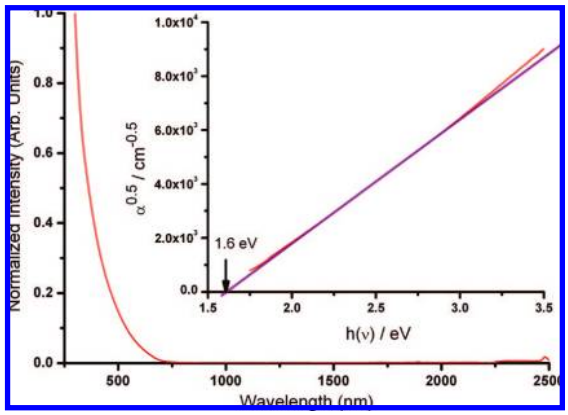

Figure 2. SnS absorption profile (NC diameter ≈ 7 nm, OA/OLA 1:1) with the square root of the absorption coefficient plotted as a function of energy (inset), displaying a linear trend for an indirect transition.

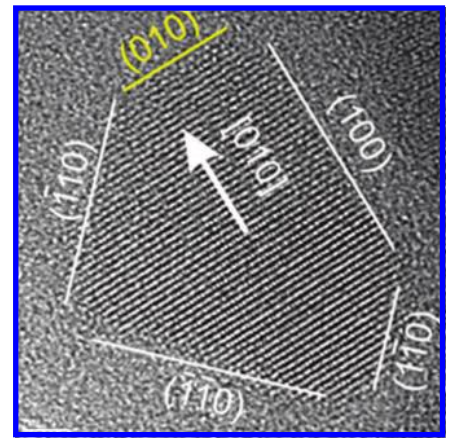

Figure 3. HRTEM depicting the termination facets of the triangular nanocrystals.

Sn and S atoms exposed to the vacuum (see Figure 3). Only the {010} facets, marked yellow in Figure 3, are composed solely from a single atom species (Sn or S). These predominant {110} and {100} terminations may be directly attributed to the growth process, if one assumes a comparable feed stock of both Sn and S atoms during the growth. In contrast, the alternating growth of facets composed of purely Sn and S layers along [010] (i.e., by subsequent termination of the particle with (010) facets) is much more unlikely. This argumentation also holds, if the facets are not parallel to the electron beam, as previously assumed, but are rather inclined by an unknown angle such that the visible particle borderlines are intersections of facets rather than facets themselves. However there are also a small number of peaks in the XRD which indicate the presence of a zinc blende structure which has previously been observed,[19] and which gains strong confirmation from the observation of a number of tetrahedral-type particles which are observed in the electron microscopy images (see Supporting Information SI 2b). These tetrahedral-type particles are larger (∼20 nm) and have a fainter contrast thus indicating a different composition (with a lower *Z*-value on average) and therefore possibly structure. The extra peaks at 29 and 33 2θ in the XRD are associated with SnO which may be expected to form at the surface of the nanocrystals over time. In the HRTEM studies no evidence for defects or the presence of impurities has been observed nor were any observed in the Energy dispersive X-ray spectroscopy (EDX) spectra. The FFT diffractograms of the HRTEM confirm the XRD patterns (see Supporting Information SI 3). High resolution TEM clearly attests to the crystallinity which is further supported by the size determined from the broadening of the X-ray diffractograms where a mean crystallite size of 7 nm was derived from the reflections using the Debye−Scherrer equation. EDX has determined the stoichiometry of the nanoparticles as being slightly enriched in sulfur.

It is expected that competitive absorption of monomer and ligands for different facets will result in an alteration in the rate of growth of the facets. Hence at high monomer concentration, relative differences between the growth rates of different facets can lead to anisotropic shapes.[20] The relative growth rates of the different facets may also be controlled by suitable variation of the ratio of the surfactants,[21] and it has been demonstrated that nonspherical geometries can result and form long-range ordered arrays.[22] In this study shape control of the SnS nanoparticles was undertaken by altering the OA/OLA ratio. Starting from spherical particles (Figure 1 left, OA/OLA 1:2), when the concentration of the carboxylic acid was increased, for any one temperature, the particle size was found to increase while at the same time the particles became more angular. The alteration in shape was found to go through an intermediate stage where, although the nanoparticles may be said to have remained monodisperse, the particle geometry is more difficult to define. They are angular and appear to be approximately bipyrimidal in shape but there are a number of particles that have a starlike appearance (see Supporting Information SI 2b,c). At higher concentrations of oleic acid the particles have a distinct triangular or truncated triangular projection with angles of 60° being prominent (Figure 1, right, OA/OLA 1:1).

The optical absorption of clear solutions of the nanocrystals, both spherical and angular, gave a scattering curve-type response even though the material is quite monodisperse, small, and nonscattering in nature (see Supporting Information SI 4). It is noted that it is certainly possible to achieve a distinct $1S_e-1S_h$ transition in the absorption profiles of the II−VI as well as the IV−VI lead chalcogenide materials of a similar size distribution. SnS has both a direct and indirect bandgap with the expected direct transition at 1.295 eV (956 nm) and the indirect at 1.095 eV (1132 nm) in the bulk material, and it is at energies greater than these that the absorption curve is observed to steeply rise for the nanocrystal samples. A graph of absorbance coefficient versus energy for the nanocrystals results in a straight line plot when $\alpha(h\nu)^{0.5}$ is employed as the abscissa suggesting that the absorbance is due to an indirect transition (Figure 2 inset). A similar behavior has previously been reported for SnS[23] and also for Si nanoparticles,[24] which also possess a direct and an indirect bandgap, and is not intuitively expected. One explanation, in the case of tin(II) sulfide, may be that as bulk SnS has both direct and indirect band gaps that are energetically quite close (0.2 eV), and whose relative positions with respect to each other under conditions of quantum confinement are as yet undetermined, the possibility of the bandgaps shifting and overlapping in energy with the consequent mixing of energetic states or even subsequently crossing over each other cannot be discounted. However, one also cannot at this juncture, discount the possibility of surface state effects, and the true nature of this absorbance profile is currently under investigation.

To assess the suitability of the nanocrystals as optically active centers for their incorporation into optoelectronic devices, a monolayer of particles was deposited onto mercaptopropionic acid derivatized ITO substrates, and their photoelectrochemical response was assessed under conditions of illumination using an LED whose peak intensity (λ_{pk} = 470 nm) is greater than

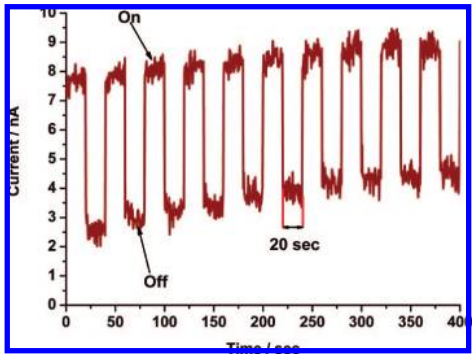

Figure 4. Photocurrent response of a submonolayer of SnS nanoparticles on an ITO substrate in 0.1 M sodium sulfate as electrolyte. $E_{app} = 800$ mV vs Ag/AgCl/3 M NaCl, area = 0.72 cm^2 (photocurrent = 6.5 nA cm^{-2}).

the calculated bandgap (see Supporting Information for further details of the deposition strategy and the conditions employed for the electrochemistry). As can be seen from Figure 4, upon illumination of the SnS-derivatized electrode the current is observed to quickly increase and remain relatively constant during the illumination time, here 20 s, and upon switching off of the LED the current returns to its preillumination value. This photocurrent response profile is reproducible over many cycles (in a number of trials for periods in excess of an hour) and an average photocurrent (current under illumination minus background current) for a number of similarly prepared electrodes has yielded values of between 6 and 8 nA cm^{-2}. It may also be expected that the photoelectrochemical response from the spherical nanocrystals may differ from that of the triangular nanocrystals, and therefore to determine if this is the case two electrodes were prepared under similar conditions. The absorbance of the two SnS NP solutions was adjusted such that they were equal at the peak intensity of the blue LED in order to obtain similarly concentrated solutions for the deposition. The concentrations are expected to be similar but not be equal as nanoparticles of the same material but different geometries are expected to possess different absorption cross-sections. Upon comparison of the photocurrent responses no discernible differences were observed (see Supporting Information SI 7). The difference in photocurrent intensities may be ascribed to differences in particle surface densities or due to the aforementioned differences in absorbance. It is also of interest that the absorbance spectra for spherical and triangular nanoparticles of similar size do not much differ from each other except at the higher energy end of the spectra (see Supporting Information SI 8) and both geometries result in a linear response for plots of the square root of the absorption coefficient versus the energy (Figure 5).

In summary we report the synthesis and characterization of monodisperse SnS nanocrystals and demonstrate shape control. Further, the ability to link the nanocrystals to conducting substrates and probe their optoelectronic response has been shown. Values of the photocurrent for this system, without attempts to optimize, in the range of 6−8 nA cm^{-2} were obtained for monolayers/submonolayers.

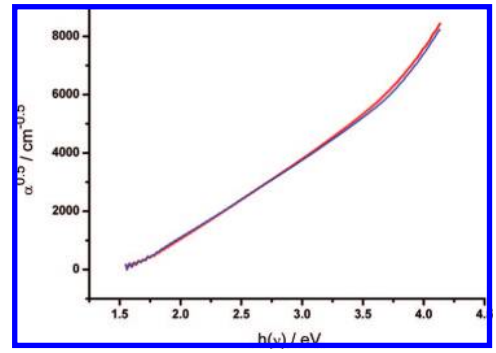

Figure 5. Square root of absorption coefficient plotted as a function of energy for spherical (red) and triangular (blue) nanocrystals.

Acknowledgment. S.G. Hickey is grateful to the Deutsche Forschungsgemeinschaft (DFG) for financial support through Grant HI-1113/3.

Supporting Information Available: Experimental details of the synthesis, XRD, FTT analysis, TEM, HRTEM, and optoelectronic measurement conditions. This material is available free of charge via the Internet at http://pubs.acs.org.

References

(1) Rogach, A. L.; Eychmüller, A.; Hickey, S. G.; Kershaw, S. V. *Small* **2007**, *3*, 536–557.
(2) Luther, J. M.; Beard, M. C.; Song, Q.; Law, M.; Ellingson, R. J.; Nozik, A. J. *Nano Lett.* **2007**, *7*, 1779–1784.
(3) Schaller, R. D.; Sykora, M.; Jeong, S.; Klimov, V. I. *J. Phys. Chem. B* **2006**, *110*, 25332–25338.
(4) Talapin, D. V.; Murray, C. B. *Science* **2005**, *310*, 86–89.
(5) Schaller, R. D.; Sykora, M.; Pietryga, J. M.; Klimov, V. I. *Nano Lett.* **2006**, *6*, 424–429.
(6) Ellingson, R. J.; Beard, M. C.; Johnson, J. C.; Yu, P. R.; Micic, O. I.; Nozik, A. J.; Shabaev, A.; Efros, A. L. *Nano Lett.* **2005**, *5*, 865–871.
(7) Murphy, J. E.; Beard, M. C.; Norman, A. G.; Ahrenkiel, S. P.; Johnson, J. C.; Yu, P. R.; Micic, O. I.; Ellingson, R. J.; Nozik, A. J. *J. Am. Chem. Soc.* **2006**, *128*, 3241–3247.
(8) Chamberlain, J. M.; Merdan, M. J. *Phys. C: Solid State Phys.* **1977**, *10*, L571–L574.
(9) Koteeswara Reddy, N.; Hahn, Y. B.; Devika, M.; Sumana, H. R.; Gunasekhar, K. R. *J. Appl. Phys.* **2007**, *101*, 093522-1–093522-7.
(10) Parenteau, M.; Carlone, C. *Phys. Rev. B* **1990**, *41*, 5227–5234.
(11) Tanuševski, A.; Poelman, D. *Solar Energy Mater. Solar Cells* **2003**, *80*, 297–303.
(12) Johnson, J. B.; Jones, H.; Latham, B. S.; Parker, J. D.; Engelken, R. D.; Barber, C. *Semicond. Sci. Technol.* **1999**, *14*, 501–507.
(13) Prince, M. B. *J. Appl. Phys.* **1955**, *26*, 534–540.
(14) Loferski, J. J. *J. Appl. Phys.* **1956**, *27*, 777–784.
(15) El-Nahass, M. M.; Zeyada, H. M.; Aziz, M. S.; El-Ghamaz, N. A. *Opt. Mater.* **2002**, *20*, 159–170.
(16) Jayalakshmi, M.; Mohan Rao, M.; Choudary, B. M. *Electrochem. Commun.* **2004**, *6*, 1119–1122.
(17) Patra, C. R.; Odani, A.; Pol, V. G.; Aurbach, D.; Gedanken, A. *J. Solid State Electrochem.* **2006**, *11*, 186–194.
(18) Kovalenko, M. V.; Heiss, W.; Shevchenko, E. V.; Lee, J. S.; Schwinghammer, H.; Alivisatos, A. P.; Talapin, D. V. *J. Am. Chem. Soc.* **2007**, *129*, 11354–11355.
(19) Greyson, E. C.; Barton, J. E.; Odom, T. W. *Small* **2006**, *2*, 368–371.
(20) Carbone, L.; Kudera, S.; Carlino, E.; Parak, W. J.; Giannini, C.; Cingolani, R.; Manna, L. *J. Am. Chem. Soc.* **2006**, *128*, 748–755.
(21) Sapra, S.; Poppe, J.; Eychmüller, A. *Small* **2007**, *3*, 1886–1888.
(22) Houtepen, A. J.; Koole, R.; Vanmaekelbergh, D. L.; Meeldijk, J.; Hickey, S. G. *J. Am. Chem. Soc.* **2006**, *128*, 6792–6793.
(23) Koktysh, D. S.; McBride, J. R.; Rosenthal, S. J. *Nanoscale Res. Lett.* **2007**, *2*, 144–148.
(24) Littau, K. A.; Szajowski, P. J.; Muller, A. J.; Kortan, A. R.; Brus, L. E. *J. Phys. Chem.* **1993**, *97*, 1224–1230.

JA8048755